The thymus regulates skeletal muscle regeneration by directly promoting satellite cell expansion

Yan-Yan Zheng[1,‡], Ye Wang[1,‡], Xin Chen[1,‡], Li-Sha Wei[1], Han Wang[1], Tao Tao[1], Yu-Wei Zhou[1], Zhi-Hui Jiang[1], Tian-Tian Qiu[1], Zhi-Yuan Sun[2], Jie Sun[1], Pei Wang[1], Wei Zhao[1], Ye-Qiong Li[1], Hua-Qun Chen[2,*], Min-Sheng Zhu[1,*], and Xue-Na Zhang[1,3,*]

From the [1]State Key Laboratory of Pharmaceutical Biotechnology, Model Animal Research Center of Medical School and Gulou Hospital Affiliated Medical School, Nanjing University, Nanjing, China; [2]Jiangsu Key Laboratory for Molecular and Medical Biotechnology, College of Life Sciences, Nanjing Normal University, Nanjing, China; [3]Jiangsu Key Laboratory for Pharmacology and Safety Evaluation of Chinese Materia Medica, Nanjing University of Chinese Medicine, Nanjing, China

Edited by Qi Qun Tang

The thymus is the central immune organ, but it is known to progressively degenerate with age. As thymus degeneration is paralleled by the wasting of aging skeletal muscle, we speculated that the thymus may play a role in muscle wasting. Here, using thymectomized mice, we show that the thymus is necessary for skeletal muscle regeneration, a process tightly associated with muscle aging. Compared to control mice, the thymectomized mice displayed comparable growth of muscle mass, but decreased muscle regeneration in response to injury, as evidenced by small and sparse regenerative myofibers along with inhibited expression of regeneration-associated genes *myh3*, *myod*, and *myogenin*. Using paired box 7 (Pax7)-immunofluorescence staining and 5-Bromo-2′-deoxyuridine-incorporation assay, we determined that the decreased regeneration capacity was caused by a limited satellite cell pool. Interestingly, the conditioned culture medium of isolated thymocytes had a potent capacity to directly stimulate satellite cell expansion *in vitro*. These expanded cells were enriched in subpopulations of quiescent satellite cells (Pax7^{high}MyoD[low]E-dU[pos]) and activated satellite cells (Pax7^{high}MyoD[high]EdU[pos]), which were efficiently incorporated into the regenerative myofibers. We thus propose that the thymus plays an essential role in muscle regeneration by directly promoting satellite cell expansion and may function profoundly in the muscle aging process.

The thymus originates from endodermal cells of the ventral third–pharyngeal pouches and then differentiates into thymic epithelial cells (TECs) and other types of thymus cells (1–4). The thymus provides proper environments for immune cell maturation, differentiation, and function; for example, medullary TECs regulate central tolerance and the development of T regulatory and natural killer T cells (2), and cortical TECs regulate positive and negative selection (5, 6). The thymus is thus considered the central lymphoid organ for the production of a diverse repertoire of immune cells. However, the thymus involutes with age and displays progressive declines in mass and function (7–9). It has been documented that this involution is closely associated with immunological aging processes such as declining naïve T cell output, alterations in T cell functions, and immunosenescence (5, 10, 11). As skeletal muscle wasting during aging parallels thymus involution (12, 13), we hypothesized that the thymus may play a role in muscle aging or related processes.

Skeletal muscle is generated during embryonic development, grows during postnatal development, and wastes during aging (14). In a developing embryo, progenitors of mesoderm-derived structures generate muscle fibers. Once the muscle has matured after birth, these progenitors, such as satellite cells, enter quiescence and reside in the sarcolemma (15). Simultaneously, the matured muscle increases its mass through myofiber hypertrophy (16). As age increases, the muscle undergoes progressive age-related atrophy, as evidenced by the shrinkage of myofibers and imbalance of protein degradation and biosynthesis (17, 18). The decreased regenerative capacity has been believed to be closely associated with skeletal muscle aging. Although the regeneration processes are regulated by multiple factors, the numerical and functional impairments of muscle-resident satellite cells are regarded as causative factors of regeneration decline or muscle aging (19, 20). In resting muscle, quiescent satellite cells (paired box 7 (Pax7^{+})MyoD[−]) are located at the sarcoplasmic membrane (21–23). When the muscle is injured, satellite cells within the injured site are activated (Pax7[+-]MyoD[+]) and sequentially differentiate into proliferative (Pax7^{−}MyoD[+]) and terminal myoblasts (MyoG[+]) before fusing into myotubes (24, 25). During this process, the activated satellite cells also produce quiescent satellite cells through asymmetric division and then return to sarcoplasmic niches (26, 27). It has been documented that the functionality of the satellite cell pool may be regulated by cell-intrinsic and circulatory factors (28). In particular, recent reports have suggested that skeletal muscle regeneration or satellite cell pool maintenance may be regulated by immune cells,

including lymphocytes and macrophages, and by thymus-associated immunity (29–31). We thus hypothesize that the thymus may serve as an essential organ for regulating skeletal muscle regeneration and aging. In this study, we used thymectomized mice and found that the thymus was necessary for satellite cell pool maintenance and muscle regeneration. Importantly, thymocyte culture medium significantly promoted satellite cell amplification, implying a remote regulatory mechanism of the thymus. Our results reveal a novel role of the thymus in skeletal muscle regeneration that links thymus involution with muscle aging.

Results

The thymus is necessary for skeletal muscle regeneration

To investigate the role of the thymus in muscle growth, we removed the thymus from adult mice according to a previously reported protocol (32–34). Four months after the operation, the mice showed reduced body weights compared to those of control mice (with sham operation), but the lean weights were comparable ($p > 0.05$) (Fig. 1A). Seven and 8 months after the operation, both the body weights and lean weights of the thymectomized mice were restored to control levels (Fig. 1, B and C), and the histological structures of the muscles were also comparable among all groups (Fig. 1D). This result showed that thymus removal did not apparently inhibit the growth of skeletal muscle mass.

To determine whether the thymus plays a role in skeletal muscle regeneration, we used the same animal model and injected the tibialis anterior (TA) muscles of C56BL/6 mice with 1.2% $BaCl_2$ solution, a widely used chemical reagent for experimental muscle injury that induces muscle depolarization and myofiber death (35, 36). Without $BaCl_2$ injection, the mice with thymus removal had no alterations in their TA muscle weights (Fig. 1E). However, upon injection with $BaCl_2$, thymus removal led to a significant increase in TA muscle weight 5 days after injury (Fig. 1E). As the muscles had reduced the numbers of regenerated fibers (with central nuclei) and edema alterations (Fig. 1, F–H), the muscular regeneration of thymectomized mice appeared impaired. We also applied cardiotoxin to repeat the above regeneration experiment and observed similar results (Fig. S1).

Regeneration of skeletal muscle after injury induces hierarchical expression of myogenic regulatory factors, including MyoD, myogenin (MyoG), and embryonic/developmental myosin heavy chain (eMHC) (37, 38). To further validate the decreased regeneration after thymus removal, we measured these myogenic markers of injured skeletal muscle. The TA muscles of thymectomized mice without $BaCl_2$ injury did not express eMHC in the same manner as the control muscles (Fig. 2A). After $BaCl_2$ injury, however, the ratio of $eMHC^+$ fibers within the injured muscles was significantly lower than that within the control muscles, and the average fiber size was also smaller (Fig. 2, A–C). In addition, we measured regeneration-associated genes such as *myh3*, *myod*, and *MyoG* and observed significantly reduced levels of both mRNA and

protein (Fig. 2, D–H). Taken together, these findings suggest that thymus removal leads to a reduced regeneration ability of skeletal muscle.

The thymus regulates the satellite cell pool during skeletal muscle regeneration

Pax7 is a specific transcription factor expressed in satellite cells and is widely used as a specific marker of satellite cells (39–41). We assessed the satellite cell pool in the injured muscle by measuring Pax7 protein and mRNA. Without $BaCl_2$ treatment, the muscles from both control and thymectomized mice had a few satellite cells ($Pax7^+$), similar to the situation in the sham-operation group (Fig. 3, A and B). After injury with $BaCl_2$ treatment, however, the number of satellite cells within the injured muscles of control mice significantly increased, whereas the number of satellite cells in the muscles of thymectomized mice increased only slightly (Fig. 3B). Measurements of *pax7* mRNA in the regenerating muscle showed a consistent result (Fig. 3C). This result indicated that the removal of the thymus significantly reduced the satellite cell pool in response to injury. We also labeled proliferating cells with 5-Bromo-2′-deoxyuridine (BrdU) after $BaCl_2$ injury and found that the number of BrdU-positive ($BrdU^+$) nuclei within regenerated muscle was significantly reduced after thymectomy (Fig. 3, D and E). This also supported the above conclusion.

Thymus cell culture directly promotes satellite cell amplification *in vitro*

The reduced satellite cell pool of thymectomized mice prompted us to speculate that active factors are released from the thymus. As previous reports have shown that concanavalin (ConA)-stimulated T cells are capable of promoting satellite cell proliferation by releasing cytokines (IL-2, IL-10, TNFα, and IFNγ) (42, 43), we cultured rat thymus cells *in vitro* for 48 h with or without activation by ConA and collected unactivated thymocyte-conditioned medium (TCM) and activated TCM (TCM-ConA). When cultured with TCM for 5 days, the satellite cells started to grow rapidly in small spheres (cell aggregates). However, when cultured with TCM-ConA, the cells grew relatively slow, and several cells adhered to the plate, showing a typical morphology of differentiated cells (Fig. 4A). This observation showed that Con-A activation of thymic lymphocytes was not necessary for satellite cell expansion. To quantify the growth of satellite cells, a Cell Counting Kit-8 assay was used. The results showed that, in contrast to basal medium, TCM significantly accelerated cell growth (Fig. 4B). To determine whether the TCM displayed comparable activity in promoting the expansion of satellite cells in different types of muscles, we isolated satellite cells from soleus (slow-twitch) and extensor digitorum (fast-twitch) muscles and then cultured them with TCM. The results showed that both types of satellite cells had the same response to TCM (Fig. S2). We next examined the amplified satellite cells by measuring Pax7 expression and found that the satellite cells
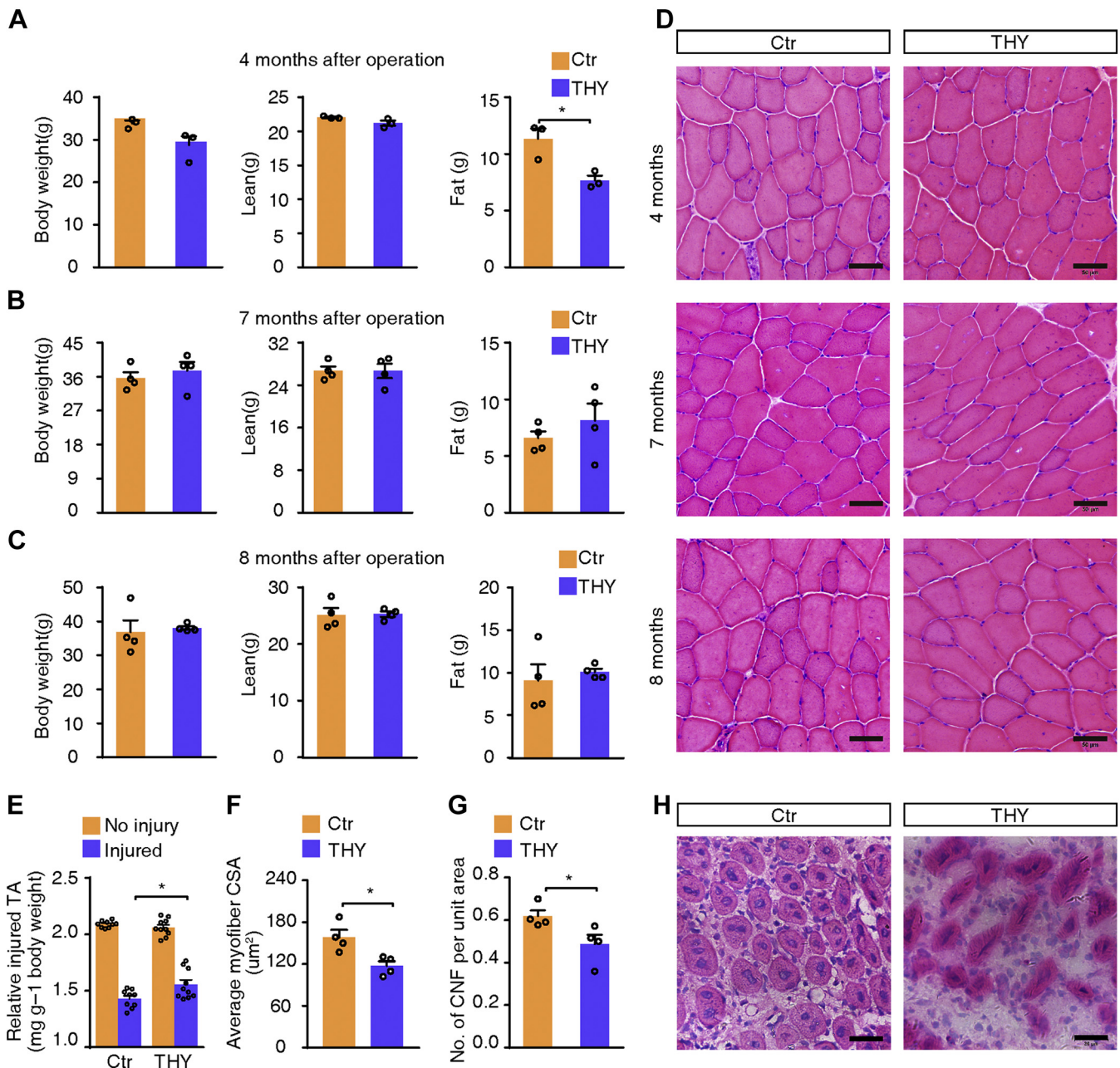
Figure 1. The thymus is necessary for skeletal muscle regeneration but not growth. *A*, the body weight, lean mass, and fat mass of control and thymectomized mice were measured at 4 months after the operation (n = 3). *B*, the body weight, lean mass, and fat mass of control and thymectomized mice were measured at 7 months after the operation (n = 4). *C*, the body weight, lean mass, and fat mass of control and thymectomized mice were measured at 8 months after the operation (n = 4). *D*, representative H&E-stained sections illustrating the histology of uninjured tibialis anterior (TA) muscles. The scale bars represent 50 μm. *E*, the uninjured TA weights and injured TA weights from the control and thymectomized groups 5 days after injury. n = 9 for control groups and n = 10 for thymectomized groups. *F*, quantification of the average cross-sectional area (CSA) of regenerating myofibers. *G*, number of myofibers containing two or more centrally located nuclei per field at day 5 postinjury. *H*, representative images of H&E-stained sections illustrating a severe regeneration defect in injured TA muscles of thymectomized mice. The scale bars represent 20 μm (n = 4). The data are presented as the mean ± SEM as determined with Student's unpaired test. *$p < 0.05$. CNF, centrally nucleated fiber; Ctr, control mice with sham operation; THY, mice with thymus removal.

continuously cultured in both conditioned mediums had remarkable increases in the percentages of Pax7-positive(Pax7$^+$) cells (Fig. 4, *C* and *D*). This observation indicated that TCM was able to promote satellite cell expansion and maintain stemness.

To measure the effects of TCM and TCM-ConA on long-term-cultured satellite cells, we mildly digested the cell aggregates and reinoculated the cells into fresh mediums.

Compared to the basal medium, both TCM and TCM-ConA accelerated cell expansion (Fig. 4, *E* and *F*). Upon culture with TCM for two passages, approximately 40% of the satellite cells were Pax7^{high}MyoD^{low} (expressing a high level of Pax7 and a low level of MyoD), 10% were Pax7^{high}MyoD^{high}, and 50% were Pax7^{low}MyoD^{low} or Pax7^{low}MyoD^{high}. In contrast, when the cells were cultured with TCM-ConA for 5 days, almost no Pax7^{high}MyoD^{low} satellite cells could be detected
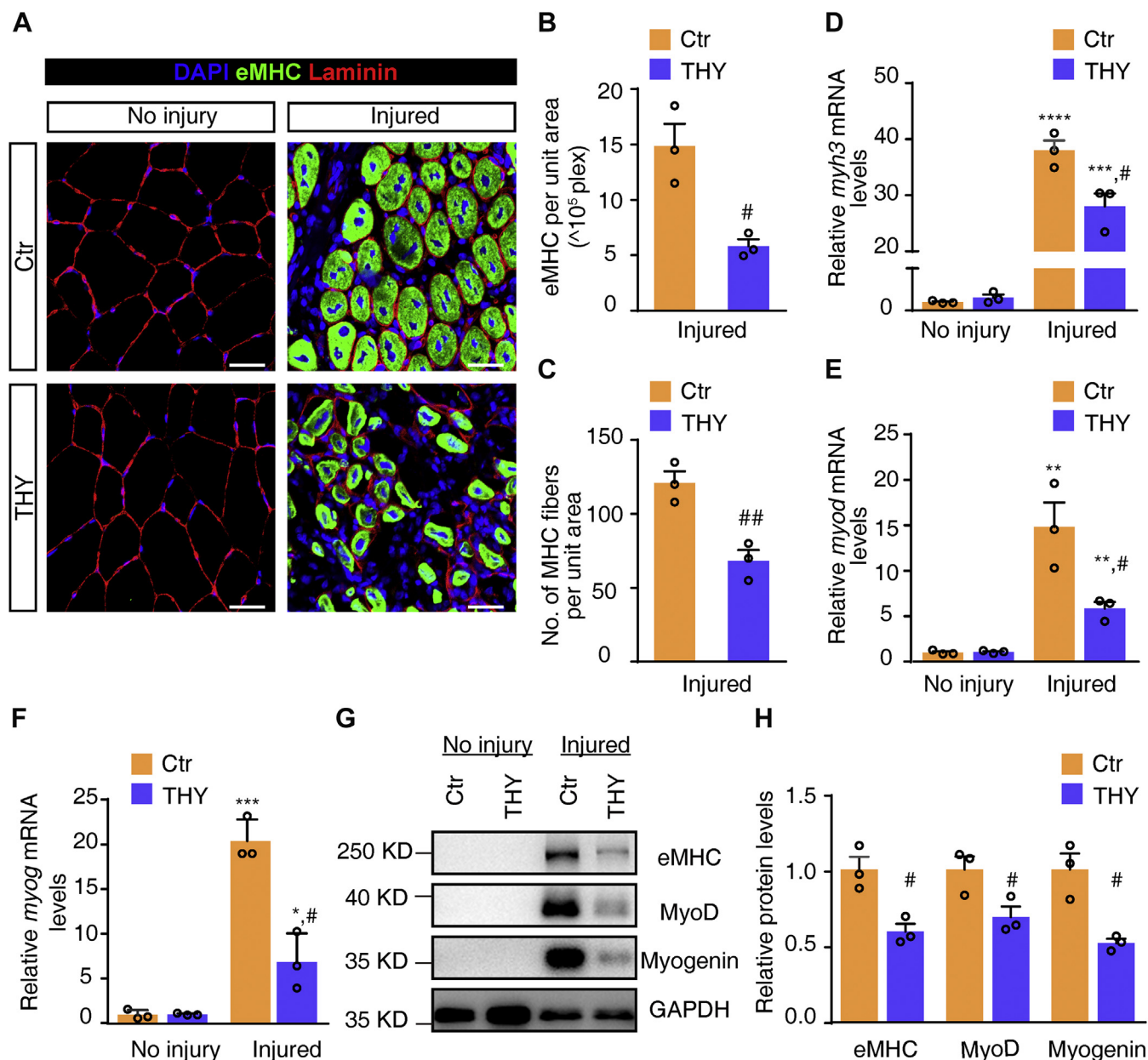
Figure 2. Thymus removal inhibits muscular regeneration and the expression of myogenic regulatory factors after injury. *A*, representative expression of eMHC (*green*) and laminin (*red*) in TA muscles 5 days after injury and uninjured TA muscle sections of control and thymectomized mice (n = 3, and each n was composed of 2–3 mice). Nuclei were identified by staining with DAPI (*blue*). The scale bars represent 100 plex. *B*, quantitation of the eMHC$^+$ staining area per unit area (n = 3). *C*, number of eMHC$^+$ myofibers per unit area (n = 3). *D*, the relative mRNA levels of *myh3* in TA muscles were measured by qRT–PCR (n = 3). *E*, the relative mRNA levels of *myod* in TA muscles were measured by qRT–PCR (n = 3). *F*, the relative mRNA levels of *myog* in TA muscles were measured by qRT–PCR (n = 3). *G*, protein measurements of eMHC, MyoD, myogenin, and GAPDH in uninjured muscles and injured muscles (n = 3). *H*, quantitation of the protein levels (n = 3). The data are the mean ± SEM. *$p < 0.05$, **$p < 0.01$, and ***$p < 0.001$, values significantly different from corresponding uninjured TA muscles of control or thymectomized mice, as determined by unpaired *t* test. #$p < 0.05$, ##$p < 0.01$, values significantly different from the corresponding injured TA muscles of thymectomized mice, as determined by paired *t* test. Ctr, control mice with sham operation; eMHC, embryonic/developmental myosin heavy chain; myog, myogenin; TA, tibialis anterior; THY, mice with thymus removal.

(Fig. 4, *G* and *H*), indicating that TCM-ConA was unable to maintain the stemness of satellite cells properly.

As Pax7^{high}MyoD^{low} cells represent the unactivated satellite cells, we then tested their dividing ability by staining with EdU. To our surprise, up to 15% of total cells were Pax7^{high}MyoD^{low}EdU^{pos} (expressing a high level of Pax7 and a low level of MyoD and EdU) (Fig. 5), indicating that Pax7^{high}MyoD^{low} cells amplified by TCM had potent division ability. In addition, we isolated fresh extensor digitorum longus myofiber explants and cultured them for 2 days to allow satellite cells to grow on *in situ* fibers. The cell number of the Pax7^{high}MyoD^{high}EdU^{pos} subpopulation cultured in TCM was also higher than that in control medium (Fig. S3).

Because splenic lymphocytes have been reported to have the potential to regulate satellite cell proliferation (44), we also
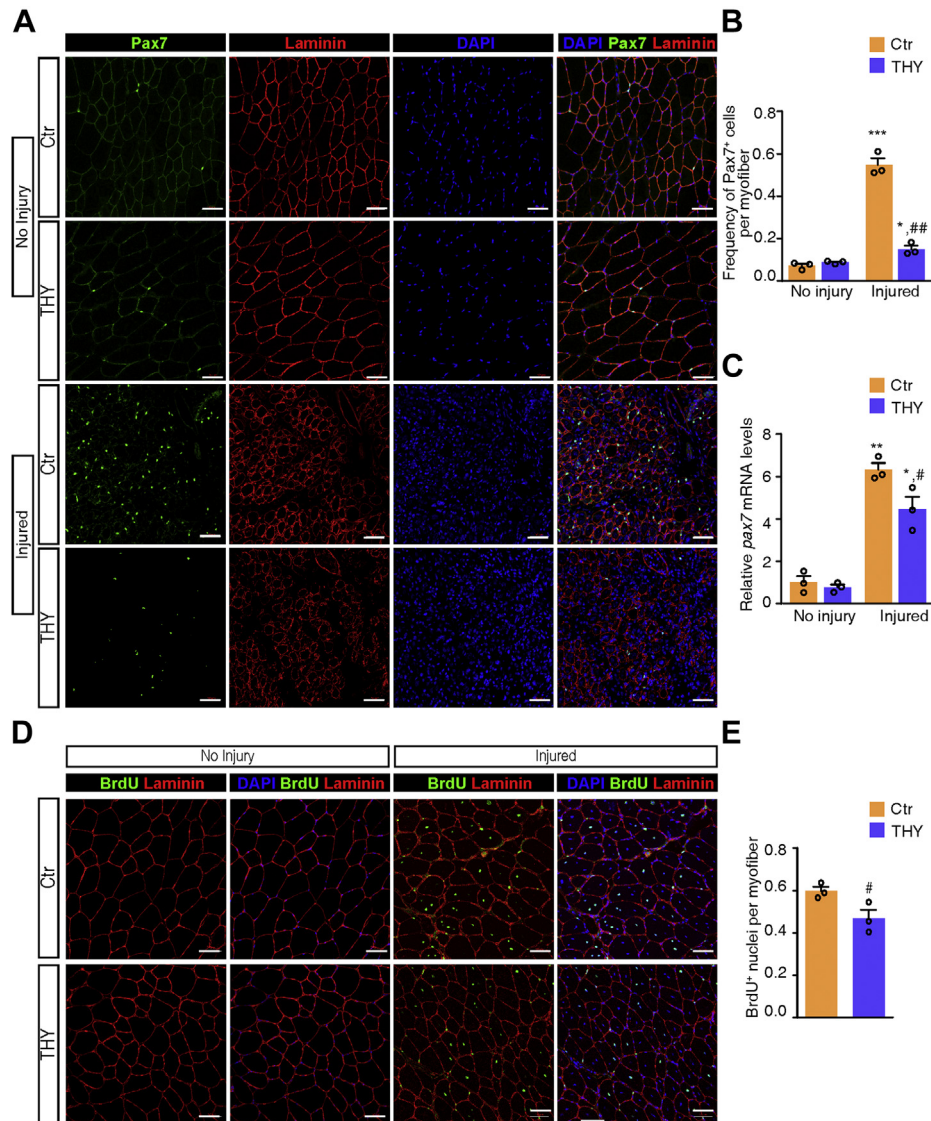
Figure 3. Thymus removal leads to a reduction in the satellite cell pool in injured skeletal muscle. *A*, representative images of Pax7 (*green*) and laminin (*red*) staining in TA muscles. TA muscles were injected with 1.2% $BaCl_2$ or saline alone for 5 days and subjected to immunostaining and mRNA measurement (n = 3). *B*, quantification of $Pax7^+$ cells per myofiber (n = 3). *C*, the relative mRNA levels of *pax7* were measured by q-PCR (n = 3). *D*, BrdU staining for TA muscles (n = 3). *E*, quantitation of the $BrdU^+$ nuclei per myofiber (n = 3 and each n was composed of 2–3 mice). The data are expressed as the mean ± SEM. *$p < 0.05$, **$p < 0.01$, and ***$p < 0.01$, values significantly different from the corresponding injured TA muscles of control mice. #$p < 0.05$ and ##$p < 0.01$, values significantly different from the corresponding injured TA muscles of thymectomized mice, as determined by paired *t* test. All scale bars represent 50 μm. BrdU, 5-Bromo-2′-deoxyuridine; Ctr, control mice with sham operation; Pax7, paired box 7; TA, tibialis anterior; THY, mice with thymus removal.

prepared splenocyte-conditioned medium (SCM) with or without ConA stimulation. However, both SCM and SCM-ConA showed weaker effects on satellite cell proliferation than TCM (Fig. S4, *A–C*). This was consistent with the observations from the animals with spleen removal, which showed no apparent difference in muscle regeneration (Fig. S4, *D–F*).

Thymocytes release cocktails of substances to promote satellite cell proliferation

To identify the active substance in TCM, we prepared serum-free TCM and subjected it to LC–MS/MS analysis. To

our surprise, most proteins extracted were metabolite inter-conversion enzymes, nucleic acid-binding proteins, cytoskeletal proteins, protein-modifying enzymes, and membrane traffic proteins; no cytokines were detected (Fig. 6A and Table S1). We then subjected serum-free TCM to HPLC chromatography with a DEAE-Sepharose FF column and eluted it with NaCl solution. We subjected all fractions to activity measurement, but unfortunately, all the fractions had weak activity except fraction 6, which showed modest activity (Fig. 6B). LC–MS/MS analysis for fraction 6 showed a protein pattern similar to that of total TCM (Fig. 6C). Interestingly, nicotinamide phosphoribosyl transferase, the cytokine nicotinamide phosphoribosyl transferase (also known as visfatin or
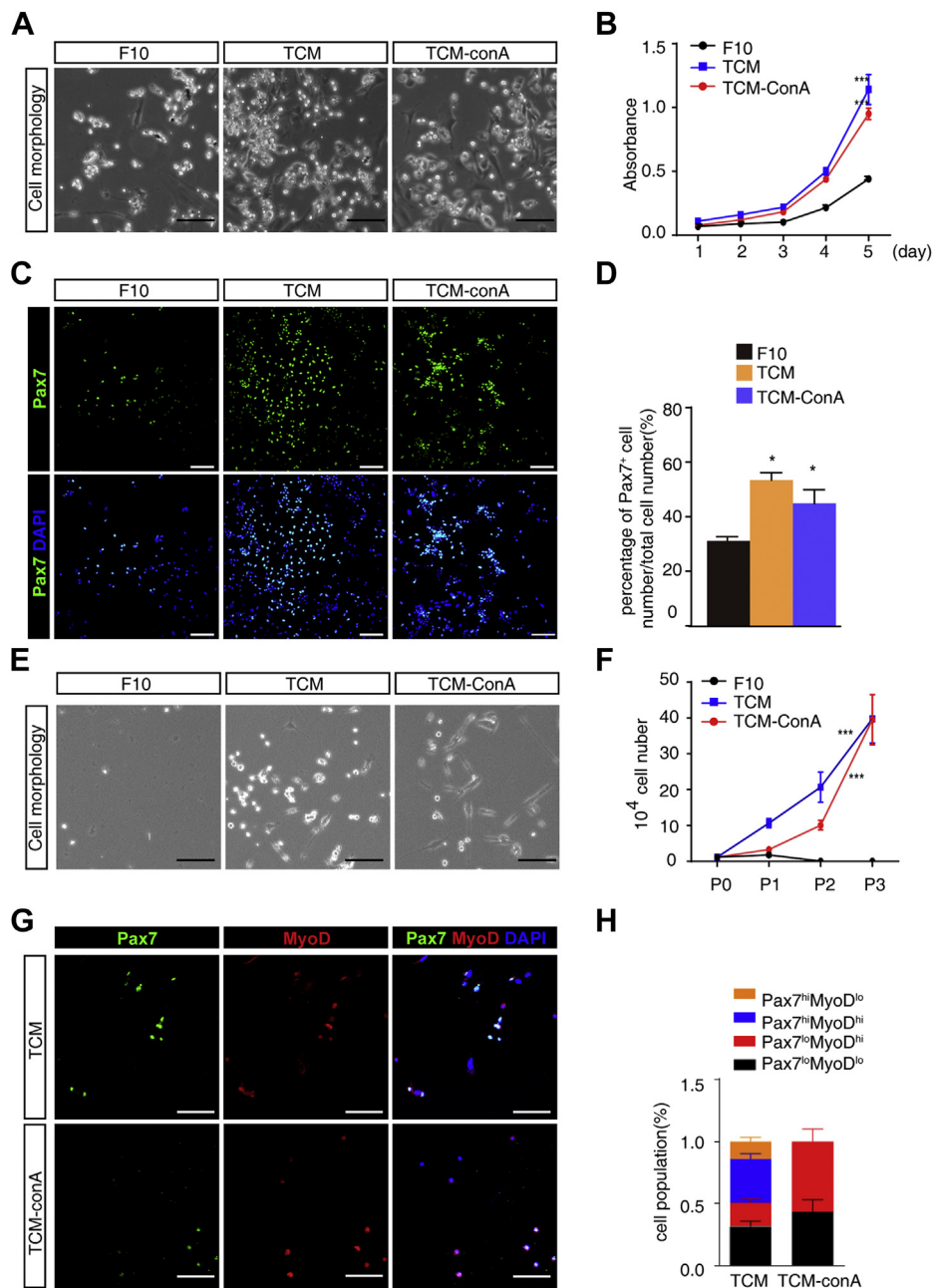
Figure 4. Thymocyte-conditioned medium promotes satellite stem cell amplification *in vitro*. *A*, satellite cell morphology cultured in different mediums for 5 days. n = 3 and each n was composed of three mice. The scale bars represent 100 μm. *B*, proliferation rate measured by CCK-8 assay. *C*, immunostaining for Pax7 (*green*) expression in satellite cells. The scale bars represent 50 μm. *D*, quantitation of Pax7$^+$ satellite cells at day 5. *E*, morphology of satellite cells (P2) cultured in different mediums. The scale bars represent 100 μm. *F*, cell numbers after amplification by different mediums over different time courses. *G*, immunostaining for Pax7 (*green*) and MyoD (*red*) expression in satellite cells. The scale bars represent 50 μm. *H*, subpopulation composition of satellite cells after 5 days of culture. TCM: medium from thymus cell without conA; TCM-conA: medium from thymus cell with conA. The data are the mean ± SEM. *$p < 0.05$ and ***$p < 0.001$. *B* and *E*, two-way ANOVA. CCK-8, cell counting kit-8; ConA, concanavalin A; Pax-7, paired box 7; TCM, thymocyte-conditioned medium.

PBEF in humans), which can act through C-C motif chemokine receptor type 5 to induce muscle–stem cell proliferation (45), was also elevated in fraction 6. To investigate the possible involvement of exosomes, we then prepared exosomes by ultracentrifugation from serum-free TCM and measured their activity toward satellite cell amplification. Moderate activity was detected for the exosome fraction (Fig. 6*D*). Collectively, the data indicate that the active presentation of thymocytes might be achieved *via* cocktails of components including exosomes.

Multiple subpopulations of thymus cells have the capacity to promote satellite cell proliferation

The thymus contains immune cells commonly expressing the CD45 antigen and CD45$^-$ nonimmune cells. To identify
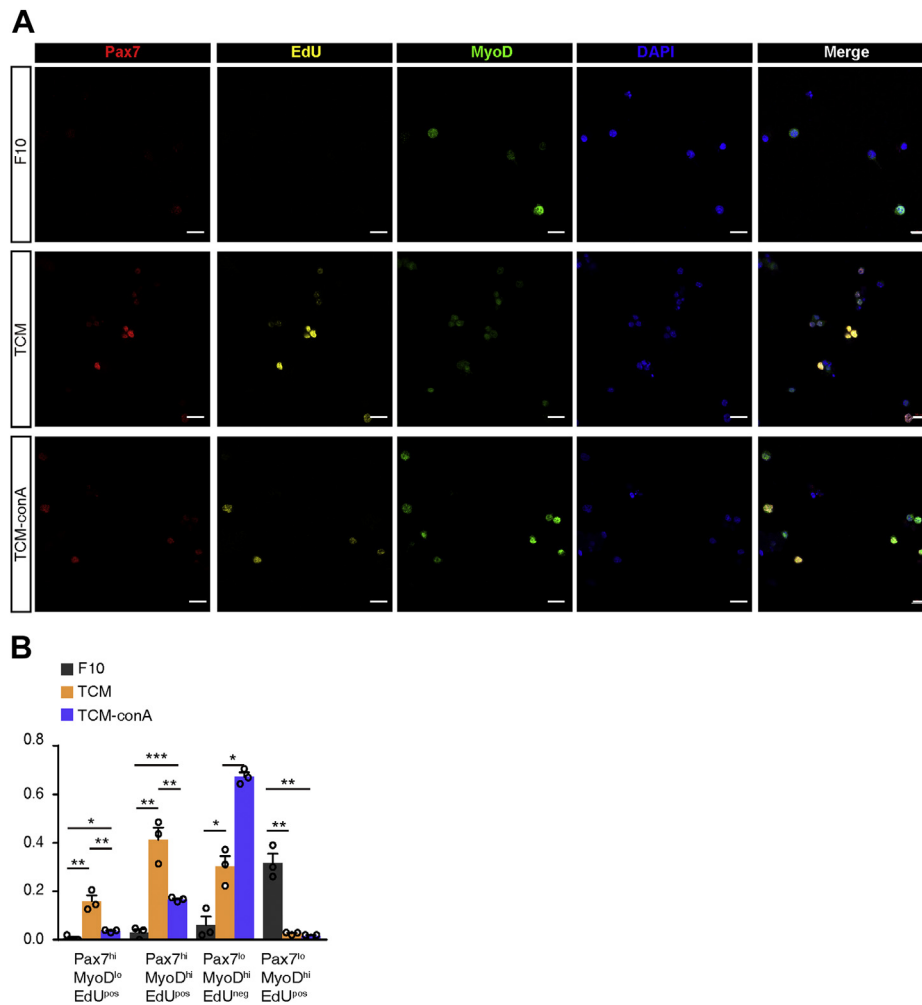
Figure 5. Effects of thymocyte subpopulations on satellite stem cell expansion *in vitro*. *A*, immunostaining of cultured satellite cells with an anti-Pax7 antibody, an anti-MyoD antibody, EdU, and DAPI. The scale bars represent 20 μm. *B*, the percentages of different cells among all cells were quantified. n = 3. The data are the mean ± SEM. Student's *t* test (two-sided): *$p < 0.05$, **$p < 0.01$, ***$p < 0.001$. ConA, concanavalin A; EdU, 5-ethynyl-29-deoxyuridine; Pax7, paired box 7; TCM, thymocyte-conditioned medium.

which population contributes to satellite cell proliferation, we separated thymus cells into three subgroups: $CD45^+CD3^+$ cells (thymic lymphocytes), $CD45^+CD3^-$ cells (thymic leucocytes except lymphocytes), and $CD45^-CD3^-$ cells (thymic non-leucocytes) by fluorescence-activated cell sorting (FACS). Among the cells, 86.8% were $CD45^+CD3^-$ cells, 9.32% were $CD45^+CD3^+$ cells, and 3.85% were $CD45^-CD3^-$ cells (Fig. 7, *A* and *B*). We adjusted lymphocytic ($CD45^+CD3^+$) and nonlymphocytic ($CD45^+CD3^-$ or $CD45^-CD3^-$) cells to the same concentration as the original cell mixture and then prepared lymphocytic TCM (TCM-L) and nonlymphocytic TCM. The results showed that both TCM-L and nonlymphocytic TCM could promote satellite cell growth, but the former promoted cell proliferation more efficiently (Fig. 7C). Among the lymphocytic thymus cells, 15.8% were $CD4^+CD8^+$ cells, 20% were $CD4^-CD8^+$ cells, 59.6% were $CD4^+CD8^-$ cells, and 0.1% were Tregs (Fig. 7, *D* and *E*). To further assess the contributions of the lymphocytic subpopulations to satellite cell proliferation, we applied equal volumes of TCM (TCM-L$CD4^+CD8^+$, TCM-L$CD4^+$, TCM-L$CD8^+$, and TCM-Treg) for satellite cell culture. TCM-L$CD4^+CD8^+$, TCM-L$CD4^+$, and TCM-L$CD8^+$

showed comparable effects on cell growth, whereas TCM-Treg showed a weak effect (Fig. 7F). This result implied that $CD4^+CD8^+$ cells had an effect comparable to those of $CD4^+CD8^-$ and $CD4^-CD8^+$ cells, and that $CD4^+CD8^+$ thymocytes might be most active in satellite cell amplification.

Satellite cells amplified by TCM efficiently incorporate the process of muscular regeneration

To assess the *in vivo* function of TCM-amplified satellite cells, we transplanted the cells into injured muscle and measured the engraftment in myofibers. Approximately, 10^5 cells from C57BL/6-EGFP mice were injected into recipient C57BL/6 TA muscles. TCM-cultured cells were harvested at the third passage, and basal medium-cultured cells were harvested at 48 h (P0) because the latter were unable to pass into P3. One day before transplantation, the recipient muscle was injected with $BaCl_2$ to initiate the regeneration process. Two months after transplantation, the incorporated enhanced green fluorescent protein-positive myofibers were measured (Fig. 8A). After transplantation with TCM-amplified cells, the
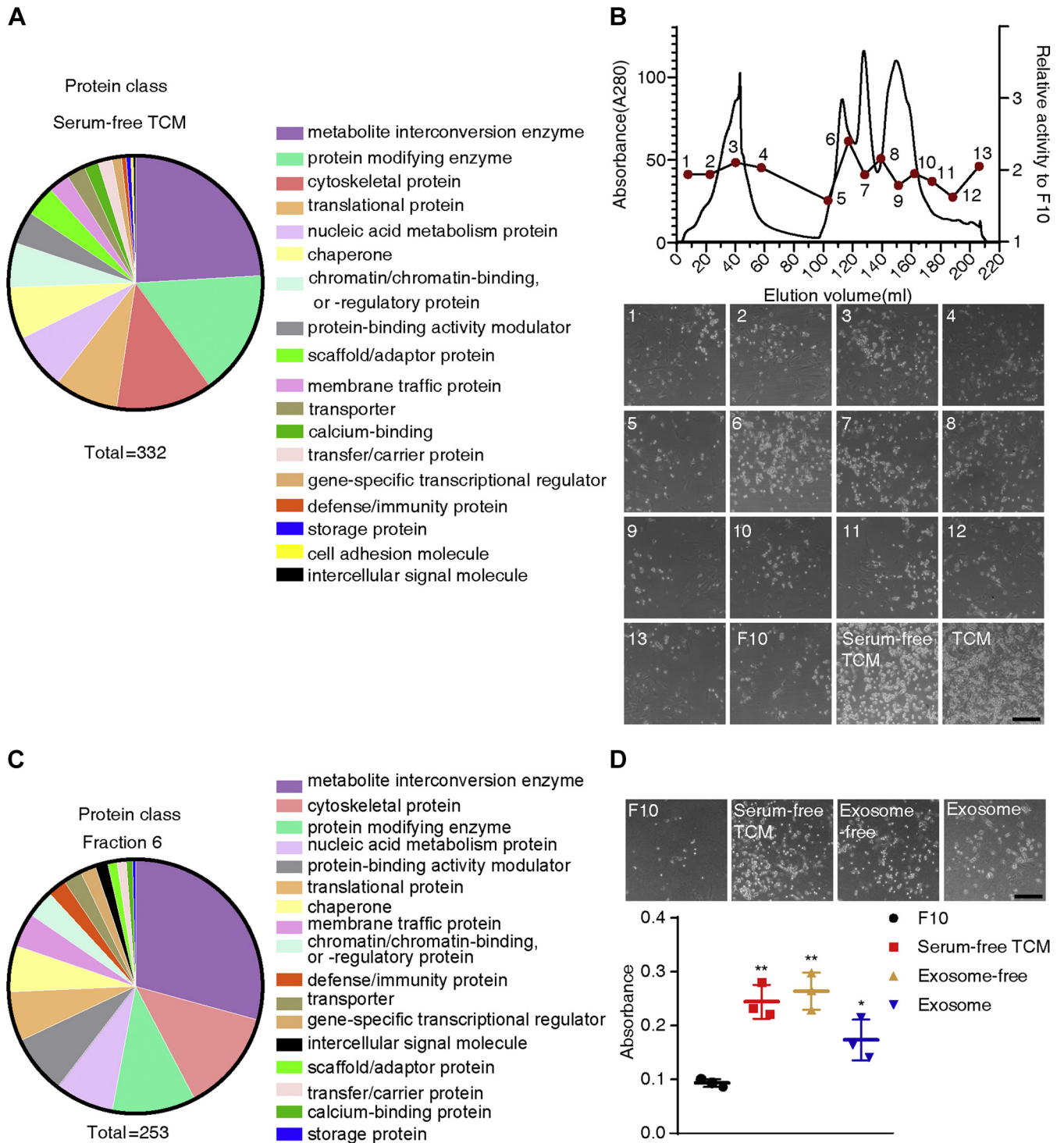
Figure 6. Active substances of TCM for satellite cell amplification. *A*, LC–MS/MS analysis of TCM. *B*, all fractions of TCM as determined by HPLC with a DEAE-Sepharose FF column and the morphology of satellite cells cultured in different fractions. The scale bars represent 200 μm. *C*, LC–MS/MS analysis of fraction 6. *D*, satellite cells were amplified by exosomes prepared from TCM. The absorbance of satellite cells cultured in basal medium (F10) was used as the control. The scale bars represent 200 μm. The data are the mean ± SEM; *$p < 0.05$, **$p < 0.01$. TCM, thymocyte-conditioned medium.

regenerated myofibers had many more EGFP-positive fibers (∼15%) than the cells cultured with basal medium (Fig. 8, *B* and *C*), suggesting that the satellite cells cultured in TCM exhibited an enhanced regeneration ability.

Given that TCM-cultured cells serve as stem cells for skeletal muscle regeneration, partially transplanted cells

should be able to locate to muscle niches and activate again when the muscle is injured once more (46). To measure the stemness of the cells, we again injured the mice that had been transplanted with TCM-cultured cells (GFP labeled) and measured the ratio of regenerated myofibers. As expected, upon second-round injury, the mice had a further increase in
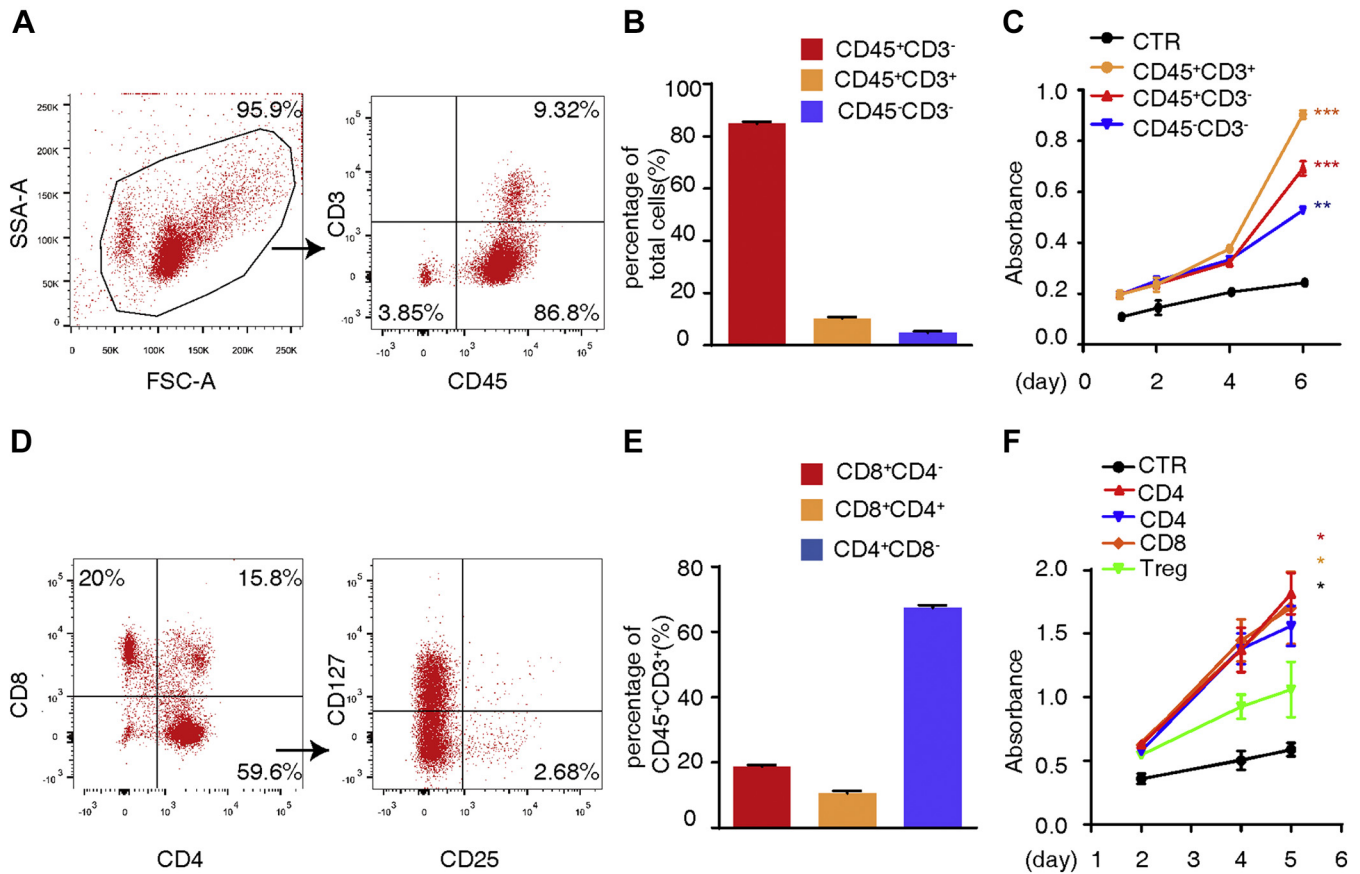
Figure 7. Effects of thymocyte subpopulations on satellite cell expansion *in vitro*. *A*, FACS analysis of three thymocyte subpopulations: CD45$^+$CD3$^+$, CD45$^+$CD3$^-$, and CD45$^-$CD3$^-$. *B*, FACS analysis was performed to separate the subpopulation of thymus cells into three groups and to determine the percentages of different cell types in the thymus. *C*, the growth rates of satellite cells in different mediums were assessed to determine the effects on proliferation by CCK-8 assay. The growth rate of satellite cells in basal medium (F10) was used as the control (CTR). *D*, the CD45$^+$CD3$^+$ subpopulation was further divided into four groups: CD4$^+$CD8$^-$ cells, CD4$^-$CD8$^+$ cells, CD4$^+$CD8$^+$ cells, and Tregs (CD4$^+$CD8$^-$CD127$^-$CD25$^+$). *E*, percentages of the cell subpopulations in the CD45$^+$CD3$^+$-subgroup cells. *F*, the growth rates of satellite cells in the different conditioned mediums prepared from four lymphocytic subpopulations were assessed to determine the effects on proliferation by CCK-8 assay. The growth rate of satellite cells in basal medium (F10) was used as the control (CTR). n = 4 and each n was composed of three mice. The data are the mean ± SEM. *$p < 0.05$, **$p < 0.01$, ***$p < 0.001$. *B* and *D*, two-way ANOVA, interaction effect. CCK-8, cell counting kit-8; FACS analysis, fluorescence-activated cell sorting.

EGFP-positive fibers (∼60%) (Fig. 8, *D* and *E*). This observation showed that satellite cells cultured with TCM have a potent capacity to replenish the endogenous stem cell pool.

Discussion

It has been well documented that the thymus is the central immune organ of the body and plays an essential role in lymphocyte development (2, 5). In this study, we found that the skeletal muscle of thymectomized animals showed significant inhibition of the regenerative response to injury along with a significant reduction in the satellite cell pool. This finding clearly suggests a novel role of the thymus in skeletal muscle regeneration. In light of the fact that declines in skeletal muscle regeneration capacity and the satellite cell pool are the major pathogenic factors of muscle aging (26, 47), the thymus may serve as an important organ inhibiting muscle aging. Because both lymphocytic (CD45$^+$CD3$^+$) and non-lymphocytic (CD45$^+$CD3$^-$) thymocytes can stimulate satellite cell proliferation by releasing factors such as exosomes, the thymus conceivably regulates this process through a remote

mechanism. In addition, because the removal of the thymus apparently does not affect muscle growth, the thymus does not affect muscular hypertrophy.

Based on our observations and current knowledge, we propose a scheme for the functional regulation of the thymus in skeletal muscle. At embryonic and postnatal developmental stages, the thymus, together with other developmental signals, promotes satellite cell proliferation to meet the needs of rapid muscle development. In adulthood, the thymus starts to involute and limit the maintenance of the satellite cell pool that displays adaptive responses to stresses imposed by pathological and aging stresses. In elderly individuals, the thymus degenerates and produces fewer secretive factors, resulting in a decline in the satellite cell pool. However, thymus involution apparently does not affect muscle mass.

The link between the thymus and skeletal muscle has been further supported by a recent report showing the involvement of thymus-derived immune cells in muscle impairment in mdx mice (30). According to our observation, this link is implemented by soluble factors and exosomes. Indeed, we identified some muscle-associated factors in TCM, for example,

ⓈⓈASBMB

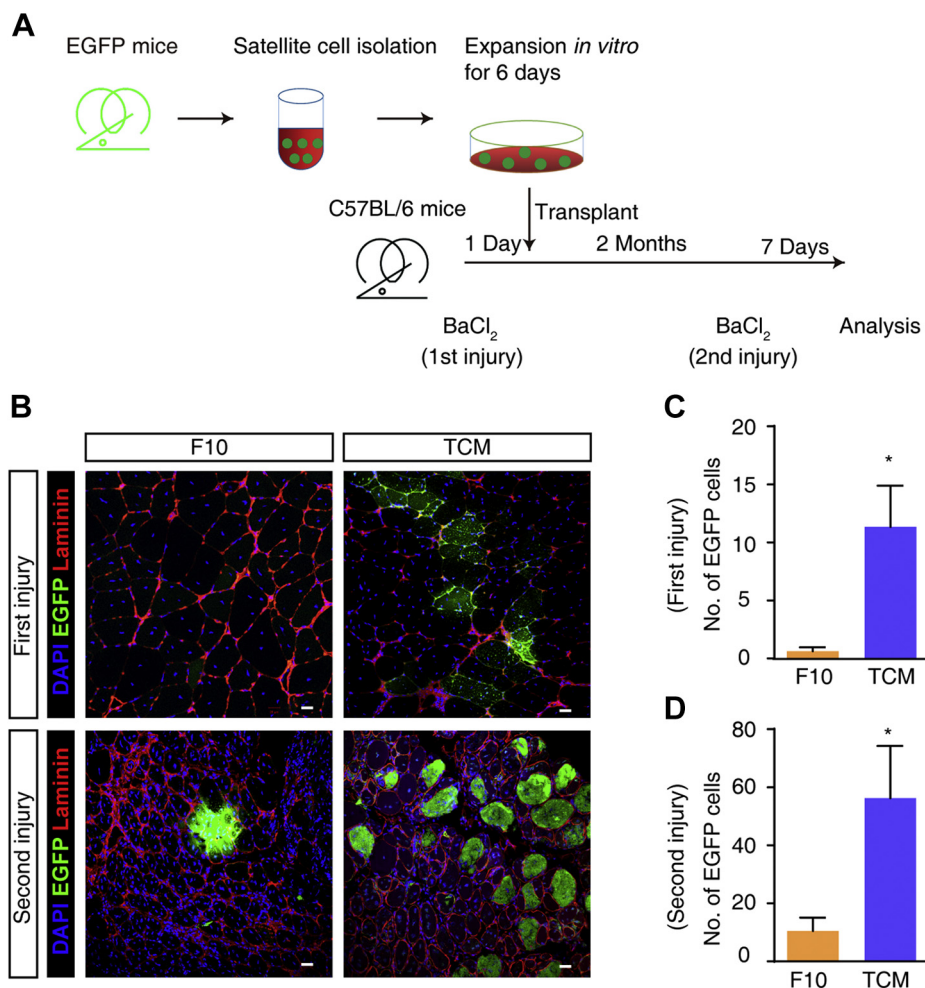*J. Biol. Chem.* (2022) 298(1) 101516 **9**

Figure 8. Amplified satellite cells efficiently incorporate into regenerated myofibers. *A*, EGFP-positive satellite cells were isolated and cultured in TCM for 6 days. Satellite cells from EGFP-transgenic mice were amplified in conditioned medium, and 10^5 cells were then transplanted into C57BL/6 mice in the injured muscles. Two months after transplantation, the muscles were injured again by $BaCl_2$ injection. The engrafted muscle was stained with an anti-EGFP antibody. Satellite cells cultured in basal medium (F10) were used as controls. *B*, representative images of regenerated myofibers with EGFP-satellite cell engraftment. *Green* indicates engrafted-EGFP$^+$ cells. *Red* indicates immunofluorescence staining of laminin. *Blue* indicates DAPI staining of nuclei. The scale bars represent 20 µm. *C*, quantitation of EGFP-positive fibers in TA muscles that received one injury. n = 3 independent experiments. *D*, quantitation of EGFP-positive fibers in TA muscles after two injuries. n = 5 independent experiments. The data are the mean ± SEM; *$p < 0.05$. TCM, thymocyte-conditioned medium.

nicotinamide phosphoribosyl transferase, a substance known to activate satellite cells (45). Identification of all of the active substances in TCM will be important in the future. Although muscle aging has a multifactorial nature, we expect that upregulating thymus function or applying active ingredients from thymus culture medium may be a promising strategy for the prevention of muscle aging or recovery of injured muscle.

Owing to the low implantation efficacy of transplanted myoblasts, transplantation of satellite cells has been regarded as a prospective method for myopathy therapy (48–52). Unfortunately, fresh satellite cells isolated from the muscle usually undergo activation and differentiation within hours *in vitro*, and how to expand enough undifferentiated satellite cells is the key challenge for transplantation therapy. Similarly, it is also a challenge for gene editing of satellite cells. According to our observation that thymus cell conditioned medium not only dramatically amplified undifferentiated satellite cells *in vitro* but also enabled the efficient incorporation of these cells into regenerating muscle *in vivo*, we may prepare

TCM and expand satellite cells isolated from adult muscles *in vitro* by approximately 10,000-fold and then conduct gene editing or cell transplantation for myopathy therapy. Our recent work indeed suggests that TCM is able to expand satellite cells from human adult muscles. Therefore, our study reveals a novel strategy for satellite cell expansion and myopathy therapy.

In summary, we have revealed a mechanistic link between the thymus and skeletal muscle regeneration or muscle aging and explored an efficient method for expanding satellite cells that is promising for myopathy therapy.

Experimental procedures

Animals

C57BL/6 (B6) and EGFP-transgenic mice (C57BL/6 background) were purchased from GemPharmatech. Thymectomy was performed according to previous reports (53, 54). The thymus lobes were removed from anesthetized mice

(8–10 weeks of age). For splenectomy, the mice were anesthetized with intraperitoneal injection of ketamine and xylazine. Then, the spleen was removed through a left subcostal incision. Sham operations were performed for the control animals. The mice were allowed to recover for 7 days before the next experiments (55). All animal procedures were performed according to the animal protocol approved by the Institutional Animal Care and Use Committee of the Model Animal Research Center of Nanjing University.

Preparation of conditioned medium

Cells from the thymus and spleen were isolated from female SD rats (200–250 g, Animal Core Facility of Nanjing Medical University) or C57BL/6 mice (GemPharmatech). Briefly, isolated thymus and spleen tissues were filtered through a 70-micron cell strainer, and red blood cells were lysed with lysis buffer. The resultant cells (1×10^7 cells/ml) were incubated in RPMI 1640 medium (RPMI 1640 supplemented with 10% fetal bovine serum (FBS), 1% L-glutamine, 1% penicillin and streptomycin, and 50 µM β-mercaptoethanol) and activated with or without 2.5 µg/ml ConA (Sigma) for 2 days. The culture medium was harvested by centrifugation, and the supernatant was used as conditioned medium. Satellite cells cultured in basal medium (F10 medium with 10% FBS and 2.5 µg/ml basic basic fibroblast growth factor) were used as the control.

q-PCR assay

Quantitative RT–PCR was performed, as described previously (56, 57). Total RNA was extracted from the tissues using RNAiso Plus (9109, Takara Bio) according to the manufacturer's instructions. The concentration and purity of the total RNA were measured at 260 nm and 280 nm using a spectrophotometer. The ratios of absorption (260/280 nm) were between 1.8 and 2.0. A total of 500 ng of RNA for each sample was reverse-transcribed with HiScript Q RT SuperMix (R123, Vazyme). Real-time PCR was performed using an ABI Prism Step-One system with AceQ qPCR SYBR Green Master Mix (R141, Vazyme). The $2^{-\Delta\Delta CT}$ method was used to analyze the relative changes in gene expression normalized against *gapdh* mRNA as an internal control. All primers are listed in Table S2.

Histological analysis

The indicated muscles were isolated and immediately frozen in isopentane, which had been cooled in liquid nitrogen in advance. The frozen muscle samples were cut into 10 µm sections and stained with H&E, as described previously (58, 59). The myofiber area was calculated and analyzed with Image-Pro Plus software. The cross-sectional area was calculated from 3 to 5 mice per group with over 200 fibers for each mouse.

Western blot analysis

Muscles were harvested at the indicated times and homogenized in ice-cold lysis buffer (2% SDS, 10 mM DTT, 10% glycerol, and 50 mM Tris–HCl, pH 7.4), containing a protease inhibitor cocktail (Roche). The homogenate was incubated at 85 °C for 5 min and stored at room temperature for 60 min. Then, the cell lysates were centrifuged at 12,000 rpm for 10 min to remove the debris. Protein was quantified with a BCA protein assay kit. The proteins were boiled at 95 °C for 5 min with sample buffer. Total protein from the skeletal muscle was loaded in one sample well for SDS/PAGE analysis. The separated proteins were transferred to a PVDF membrane (Bio–Rad). Then, the membranes were incubated with the corresponding primary antibodies overnight at 4 °C after blocking. After washing, the membranes were incubated with corresponding horseradish peroxidase-conjugated secondary antibodies (Thermo Fisher, 31460 and 31430) for 2 h at room temperature (RT). Finally, after washing in TBST, immunoreactivity was visualized using an ECL Western blotting detection system. SuperBrightSubpico ECL Substrate and Prolong ECL Substrate (Sudgen Biotechnology) were used. The antibodies were as follows: anti-MyoG (Santa Cruz Biotechnology, sc-576, 1:1000), anti-eMHC (Developmental Studies Hybridoma Bank, 1:500), anti-Pax7 (Developmental Studies Hybridoma Bank, 1:200), anti-GAPDH (Santa Cruz Biotechnology, sc-32233, 1:2000), and anti-MyoD (Santa Cruz Biotechnology, sc-377460, 1:500).

Immunofluorescence analysis

For immunofluorescence staining, cultured cells, myofibers, and muscle sections were fixed in 4% paraformaldehyde for 15 min and then permeabilized with 0.25% Triton X-100 in PBS for 15 min at RT. The nonspecific binding of primary antibodies was blocked with 1% bovine serum albumin or 5% nonimmune goat serum for 1 h. Then, the samples were incubated with primary antibodies overnight at 4 °C under humidified conditions. Pax7 staining on frozen TA muscle sections was performed according to a method described previously (46). Briefly, the muscle sections were fixed with 4% paraformaldehyde for 15 min and treated with cold methanol for permeabilization. An antigen-retrieval step was performed before blocking with Citrate Antigen Retrieval Solution (E673001, Sangon Biotech). After washing with PBS, the sections were blocked with 1% bovine serum albumin in PBST. Then, the sections were incubated with anti-Pax7 (Developmental Studies Hybridoma Bank) overnight at 4 °C. The sections were incubated with Alexa Fluor 488- or 594-conjugated secondary antibodies for 1 h at RT and then washed three times for 10 min with PBS. The nuclei were stained with DAPI together with secondary antibodies. For other immunofluorescence staining, anti-eMHC (Developmental Studies Hybridoma Bank) and anti-laminin (Sigma–Aldrich, L9393, 1:1000) antibodies were used as primary antibodies. The slides were mounted and visualized at room temperature with a Zeiss LSM880.

Muscle regeneration

Muscle regeneration was performed following a protocol described previously (60, 61). For muscle injury experiments, 100 µl of 1.2% $BaCl_2$ (Sigma) dissolved in saline was injected

into one TA muscle. The other TA muscle was injected with saline (100 µl) as a control. At the indicated time points after injection, the muscles were then harvested to evaluate the process of regeneration and repair. For one experiment, the mice were given an intraperitoneal injection of BrdU (100 µg per mouse) at day 3 and an intramuscular injection of 1.2% $BaCl_2$ (61). At the indicated time points, the TA muscles were harvested from the mice for biochemical and histological studies.

The mice used in the thymus removal experiment were 8 to 10 weeks of age. Afterward, these mice were allowed to rest for 1 week. Then, barium chloride was injected into the skeletal muscle. The mice were 9 to 12 weeks old at the time of injection.

For cardiotoxin injury, 50 µl of cardiotoxin (10 µM; Sigma–Aldrich) was injected into the TA, and an equivalent volume of PBS was injected into another limb (62–64).

Isolation of satellite cells

Satellite cells were prepared, as described previously (65). Hindlimb muscles of 6~8-week-old mice were isolated and minced to obtain a muscle suspension. The tissues were first digested with collagenase type II (700 units, Life Technologies, Gibco, catalog number: 17101-015) in Dulbecco's modified Eagle's medium (DMEM) with 5% horse serum at 37 °C on a horizontal rocking bed for 90 min. Then, the digested muscles were incubated in a second digestion with collagenase II (100 units/ml final concentration) and dispase II (2 U/ml; Roche) for 30 min with more vigorous shaking until most blocks had disappeared. The completely digested muscles were filtered through a 40-µm nylon cell strainer (Thermo Fisher) and washed to obtain mononuclear cell suspensions. The isolated cells were cultured in medium (DMEM supplemented with 10% fetal bovine serum, Gluta-MAX Supplement, and 1% penicillin–streptomycin) for 2 h at 37 °C to remove the fibroblasts. Then, the supernatant was collected and centrifuged at 300g for 5 min at RT. Muscle satellite cells were collected and cultured on collagen-coated dishes in F10 basal medium (F10 medium containing 15% FBS and 2.5 ng/ml basic fibroblast growth factor (Pepro-Tech)) and TCM (F10 medium with 15% fetal bovine serum:thymocyte medium = 1:1). The medium was replaced every other day.

Cell proliferation assay

An EdU assay was performed following the manufacturer's instructions (C10229, Thermo Scientific). Satellite cells growing on coverslips were incubated in growth medium with 10 µM EdU for the indicated times. The cells were then washed with PBS and fixed with 4% paraformaldehyde for 15 min. EdU-labeled cells were visualized with an Alexa Fluor 594-conjugated azide. Cell counting assays were conducted using a CCK-8 (20118, SUDGEN). Briefly, the cells were seeded in a 96-well plate, cultured for the indicated times, and then treated with the kit for 4 h (66). Proliferation was measured at an absorbance of 450 nm with background

subtraction at 650 nm using a microplate reader (BioTek synergy microplate reader).

For anti-BrdU staining, the frozen muscle samples were treated with 1 M HCl for 10 min on ice. Next, the samples were treated with 2 M HCl for 10 min at RT and then 20 min at 37 °C before being washed in 0.1 M $Na_2B_4O_7$ buffer at pH 8.5 (67). Then, the samples were incubated with primary antibodies overnight at 4 °C under humidified conditions after blocking.

Cell transplantation

To induce muscle injury, $BaCl_2$ (Sigma–Aldrich) was injected into the TA muscles of C57BL/6 mice (8–10 weeks) 24 h before transplantation. Independent C57BL/6-EGFP transgenic mouse-derived satellite cells cultured with basal medium (F10) or conditioned medium were injected directly into the TA muscle (68).

Isolation of thymocyte-derived exosomes

The conditioned serum-free medium from thymocytes cultured for 48 h was pooled together for exosome isolation, as described previously (69). For the ultracentrifugation method, the cellular debris was removed by centrifugation at 300g for 10 min at 4 °C followed by centrifugation at 10,000g for 30 min to remove microvesicles. Subsequently, the conditioned medium was directly centrifuged at 100,000g and 4 °C for 70 min using an Optima XPN-100 ultracentrifuge with a swinging bucket rotor. The supernatant was discarded, and the exosome pellet was resuspended in PBS and washed by ultracentrifugation at 100,000 g at 4 °C for 70 min. After this, the exosomes were resuspended in PBS and stored at –80 °C for further use.

Isolation of thymocytes and splenocytes

The thymus and spleen were dissected from mice and then ground in cold PBS. The cell suspension was filtered through a 40 µm strainer. Red blood cells were lysed with red blood cell lysis buffer (70). The rest of the cells were analyzed by FACS for cell percentages or for cell culture. For thymocyte subpopulation assays, the cells were stained with the following surface antibodies in flow cytometry staining buffer (486.5 ml of 1× PBS, 12.5 ml of goat serum, and 1 ml of 0.5 M EDTA): PE anti-mouse CD127 (BioLegend), APC anti-mouse CD25 (BioLegend), FITC anti-mouse CD4 (BioLegend), PE-Cy5.5 anti-mouse CD8 (BioLegend), PE-Cy7 anti-mouse CD3 (BioLegend), and APC-Cy7 anti-mouse CD45 (BioLegend). The cells were incubated with the antibodies above in the tubes on ice for 45 min. The different subpopulations were counted and collected by FACS sorting (BD FACSAria III).

Body composition measurements

The whole body composition was measured by using a PIXImus small animal dual-energy X-ray absorptiometry system (GE Medical System Lunar). All the mice used for detection were first anesthetized by intraperitoneal injection with ketamine and xylazine and then placed in the prone position on the specimen tray to scan the whole body.

Purification of active substance

The serum-free TCM was passed through a DEAE-Sepharose FF column using AKTA liquid chromatography systems. The column was preequilibrated with 10 mM Tris–HCl, pH 8.5, at a flow rate of 3.0 ml/min. The serum-free TCM was loaded onto the column at a flow rate of 1.0 ml/min and eluted with 1 M NaCl and 10 mM Tris–HCl, pH 8.5, at a flow rate of 1 ml/min. The column was assessed by monitoring the absorption at 280 nm. The eluted fractions from the DEAE column were divided into 13 groups. Finally, they were dialyzed and lyophilized for further analysis.

LC–MS/MS analysis

The serum-free TCM and eluted fractions were analyzed by mass spectrometry using a nanoLC.2D (Eksigent Technologies) coupled with a TripleTOF 5600+ System (AB Sciex). The peptides were eluted with a 90 min gradient of 5 to 80% mobile phase B (mobile phase A: 0.1% formic acid and 5% acetonitrile; mobile phase B: 0.1% formic acid and 95% acetonitrile) with a nanoLC column (Eksigent Technologies, 3C18-CL, 75 μm*15 cm). The data were analyzed with ProteinPilot Software (version 4.5, AB Sciex) using the UniProt database (April 9, 2018, containing 29,940 sequences, http://www.uniprot.org/proteomes/UP000002494). Corresponding protein class maps were generated with online GO software (http://geneontology.org/). The FDR threshold was specified as 1%. The mass spectrometry proteomics data have been deposited to the ProteomeXchange Consortium *via* the PRIDE partner repository with the dataset identifier PXD027407 (http://proteomecentral.proteomexchange.org/cgi/GetDataset).

Statistical analysis

Biological replicates were tested with individual mice. The p values are indicated either with numbers on the graphs or with asterisks: $*p < 0.05$, $**p < 0.01$, and $***p < 0.001$. Differences between groups were assessed by using Student's two-tailed t test for independent samples with GraphPad Prism version 6. All of the data are presented as the mean ± SEM (n ≥ 3).

Data availability

The mass spectrometry proteomics data have been deposited to the ProteomeXchange Consortium *via* the PRIDE partner repository with the dataset identifier PXD027407. http://proteomecentral.proteomexchange.org/cgi/GetDataset.

Abbreviations—The abbreviations used are: BrdU, 5-Bromo-2′-deoxyuridine; ConA, concanavalin; EdU, 5-ethynyl-29-deoxyuridine; eMHC, embryonic/developmental myosin heavy chain; FACS, fluorescence-activated cell sorting; FBS, fetal bovine serum; MyoG, myogenin; Pax7, paired box 7; SCM, splenocyte-conditioned medium; TA, tibialis anterior; TCM, thymocyte-conditioned medium; TCM-L, lymphocytic TCM; TECs, thymic epithelial cells.

References

1. Pannerec, A., Marazzi, G., and Sassoon, D. (2012) Stem cells in the hood: The skeletal muscle niche. *Trends Mol. Med.* **18**, 599–606
2. Gordon, J., and Manley, N. R. (2011) Mechanisms of thymus organogenesis and morphogenesis. *Development* **138**, 3865–3878
3. Rodewald, H. R. (2008) Thymus organogenesis. *Annu. Rev. Immunol.* **26**, 355–388
4. Boehm, T. (2008) Thymus development and function. *Curr. Opin. Immunol.* **20**, 178–184
5. Shanley, D. P., Aw, D., Manley, N. R., and Palmer, D. B. (2009) An evolutionary perspective on the mechanisms of immunosenescence. *Trends Immunol.* **30**, 374–381
6. Miller, J. (2020) The function of the thymus and its impact on modern medicine. *Science* **369**, eaba2429
7. Gui, J., Mustachio, L. M., Su, D. M., and Craig, R. W. (2012) Thymus size and age-related thymic involution: Early programming, sexual dimorphism, progenitors and stroma. *Aging Dis.* **3**, 280–290
8. van Gent, R., Schadenberg, A. W., Otto, S. A., Nievelstein, R. A., Sieswerda, G. T., Haas, F., Miedema, F., Tesselaar, K., Jansen, N. J., and Borghans, J. A. (2011) Long-term restoration of the human T-cell compartment after thymectomy during infancy: A role for thymic regeneration? *Blood* **118**, 627–634
9. Vrisekoop, N., den Braber, I., de Boer, A. B., Ruiter, A. F., Ackermans, M. T., van der Crabben, S. N., Schrijver, E. H., Spierenburg, G., Sauerwein, H. P., Hazenberg, M. D., de Boer, R. J., Miedema, F., Borghans, J. A., and Tesselaar, K. (2008) Sparse production but preferential incorporation of recently produced naive T cells in the human peripheral pool. *Proc. Natl. Acad. Sci. U. S. A.* **105**, 6115–6120
10. Aspinall, R., and Andrew, D. (2000) Thymic atrophy in the mouse is a soluble problem of the thymic environment. *Vaccine* **18**, 1629–1637
11. Aw, D., Silva, A. B., and Palmer, D. B. (2007) Immunosenescence: Emerging challenges for an ageing population. *Immunology* **120**, 435–446
12. Bamman, M. M., Roberts, B. M., and Adams, G. R. (2018) Molecular regulation of exercise-induced muscle fiber hypertrophy. *Cold Spring Harb. Perspect. Med.* **8**, a029751
13. Seene, T., and Kaasik, P. (2012) Role of exercise therapy in prevention of decline in aging muscle function: Glucocorticoid myopathy and unloading. *J. Aging Res.* **2012**, 172492
14. Musumeci, G., Castrogiovanni, P., Coleman, R., Szychlinska, M. A., Salvatorelli, L., Parenti, R., Magro, G., and Imbesi, R. (2015) Somitogenesis: From somite to skeletal muscle. *Acta Histochem.* **117**, 313–328

15. Costamagna, D., Berardi, E., Ceccarelli, G., and Sampaolesi, M. (2015) Adult stem cells and skeletal muscle regeneration. *Curr. Gene Ther.* **15**, 348–363

16. Young, V. R. (1974) Regulation of protein synthesis and skeletal muscle growth. *J. Anim. Sci.* **38**, 1054–1070

17. Wilkinson, D. J., Piasecki, M., and Atherton, P. J. (2018) The age-related loss of skeletal muscle mass and function: Measurement and physiology of muscle fibre atrophy and muscle fibre loss in humans. *Ageing Res. Rev.* **47**, 123–132

18. Larsson, L., Degens, H., Li, M., Salviati, L., Lee, Y. I., Thompson, W., Kirkland, J. L., and Sandri, M. (2019) Sarcopenia: Aging-related loss of muscle mass and function. *Physiol. Rev.* **99**, 427–511

19. Franco, I., Johansson, A., Olsson, K., Vrtacnik, P., Lundin, P., Helgadottir, H. T., Larsson, M., Revechon, G., Bosia, C., Pagnani, A., Provero, P., Gustafsson, T., Fischer, H., and Eriksson, M. (2018) Somatic mutagenesis in satellite cells associates with human skeletal muscle aging. *Nat. Commun.* **9**, 800

20. Scicchitano, B. M., Dobrowolny, G., Sica, G., and Musaro, A. (2018) Molecular insights into muscle homeostasis, atrophy and wasting. *Curr. Genomics* **19**, 356–369

21. Mauro, A. (1961) Satellite cell of skeletal muscle fibers. *J. Biophys. Biochem. Cytol.* **9**, 493–495

22. Yin, H., Price, F., and Rudnicki, M. A. (2013) Satellite cells and the muscle stem cell niche. *Physiol. Rev.* **93**, 23–67

23. Bentzinger, C. F., Wang, Y. X., and Rudnicki, M. A. (2012) Building muscle: Molecular regulation of myogenesis. *Cold Spring Harb. Perspect. Biol.* **4**, a008342

24. Wang, Y. X., and Rudnicki, M. A. (2011) Satellite cells, the engines of muscle repair. *Nat. Rev. Mol. Cell Biol.* **13**, 127–133

25. Mukund, K., and Subramaniam, S. (2020) Skeletal muscle: A review of molecular structure and function, in health and disease. *Wiley Interdiscip. Rev. Syst. Biol. Med.* **12**, e1462

26. Le Moal, E., Pialoux, V., Juban, G., Groussard, C., Zouhal, H., Chazaud, B., and Mounier, R. (2017) Redox control of skeletal muscle regeneration. *Antioxid. Redox Signal.* **27**, 276–310

27. Shinin, V., Gayraud-Morel, B., Gomes, D., and Tajbakhsh, S. (2006) Asymmetric division and cosegregation of template DNA strands in adult muscle satellite cells. *Nat. Cell Biol.* **8**, 677–687

28. Hwang, A. B., and Brack, A. S. (2018) Muscle stem cells and aging. *Curr. Top. Dev. Biol.* **126**, 299–322

29. Shang, M., Cappellesso, F., Amorim, R., Serneels, J., Virga, F., Eelen, G., Carobbio, S., Rincon, M. Y., Maechler, P., De Bock, K., Ho, P. C., Sandri, M., Ghesquiere, B., Carmeliet, P., Di Matteo, M., *et al.* (2020) Macrophage-derived glutamine boosts satellite cells and muscle regeneration. *Nature* **587**, 626–631

30. Farini, A., Sitzia, C., Villa, C., Cassani, B., Tripodi, L., Legato, M., Belicchi, M., Bella, P., Lonati, C., Gatti, S., Cerletti, M., and Torrente, Y. (2021) Defective dystrophic thymus determines degenerative changes in skeletal muscle. *Nat. Commun.* **12**, 2099

31. Panduro, M., Benoist, C., and Mathis, D. (2018) Treg cells limit IFN-gamma production to control macrophage accrual and phenotype during skeletal muscle regeneration. *Proc. Natl. Acad. Sci. U. S. A.* **115**, E2585–E2593

32. Wainwright, D. A., Sengupta, S., Han, Y., and Lesniak, M. S. (2011) Thymus-derived rather than tumor-induced regulatory T cells predominate in brain tumors. *Neuro Oncol.* **13**, 1308–1323

33. Vianna, P. H., Canto, F. B., Nogueira, J. S., Nunes, C. F., Bonomo, A. C., and Fucs, R. (2016) Critical influence of the thymus on peripheral T cell homeostasis. *Immun. Inflamm. Dis.* **4**, 474–486

34. Novoseletskaya, A. V., Kiseleva, N. M., Zimina, I. V., Bystrova, O. V., Belova, O. V., Inozemtsev, A. N., Arion, V. Y., and Sergienko, V. I. (2015) Thymus polypeptide preparation tactivin restores learning and memory in thymectomied rats. *Bull. Exp. Biol. Med.* **159**, 623–625

35. Hardy, D., Besnard, A., Latil, M., Jouvion, G., Briand, D., Thepenier, C., Pascal, Q., Guguin, A., Gayraud-Morel, B., Cavaillon, J. M., Tajbakhsh, S., Rocheteau, P., and Chretien, F. (2016) Comparative study of injury models for studying muscle regeneration in mice. *PLoS One* **11**, e0147198

36. DalleDonne, I., Milzani, A., and Colombo, R. (1998) Effect of replacement of the tightly bound Ca2+ by Ba2+ on actin polymerization. *Arch. Biochem. Biophys.* **351**, 141–148

37. Kuang, S., Kuroda, K., Le Grand, F., and Rudnicki, M. A. (2007) Asymmetric self-renewal and commitment of satellite stem cells in muscle. *Cell* **129**, 999–1010

38. Beauchamp, J. R., Heslop, L., Yu, D. S., Tajbakhsh, S., Kelly, R. G., Wernig, A., Buckingham, M. E., Partridge, T. A., and Zammit, P. S. (2000) Expression of CD34 and Myf5 defines the majority of quiescent adult skeletal muscle satellite cells. *J. Cell Biol.* **151**, 1221–1234

39. von Maltzahn, J., Jones, A. E., Parks, R. J., and Rudnicki, M. A. (2013) Pax7 is critical for the normal function of satellite cells in adult skeletal muscle. *Proc. Natl. Acad. Sci. U. S. A.* **110**, 16474–16479

40. Sambasivan, R., Yao, R., Kissenpfennig, A., Van Wittenberghe, L., Paldi, A., Gayraud-Morel, B., Guenou, H., Malissen, B., Tajbakhsh, S., and Galy, A. (2011) Pax7-expressing satellite cells are indispensable for adult skeletal muscle regeneration. *Development* **138**, 3647–3656

41. Kuang, S., Charge, S. B., Seale, P., Huh, M., and Rudnicki, M. A. (2006) Distinct roles for Pax7 and Pax3 in adult regenerative myogenesis. *J. Cell Biol.* **172**, 103–113

42. Aloud, B. M., Petkau, J. C., Yu, L., McCallum, J., Kirby, C., Netticadan, T., and Blewett, H. (2020) Effects of cyanidin 3-O-glucoside and hydrochlorothiazide on T-cell phenotypes and function in spontaneously hypertensive rats. *Food Funct.* **11**, 8560–8572

43. Fu, X., Xiao, J., Wei, Y., Li, S., Liu, Y., Yin, J., Sun, K., Sun, H., Wang, H., Zhang, Z., Zhang, B. T., Sheng, C., Wang, H., and Hu, P. (2015) Combination of inflammation-related cytokines promotes long-term muscle stem cell expansion. *Cell Res.* **25**, 1082–1083

44. Kwee, B. J., Budina, E., Najibi, A. J., and Mooney, D. J. (2018) CD4 T-cells regulate angiogenesis and myogenesis. *Biomaterials* **178**, 109–121

45. Ratnayake, D., Nguyen, P. D., Rossello, F. J., Wimmer, V. C., Tan, J. L., Galvis, L. A., Julier, Z., Wood, A. J., Boudier, T., Isiaku, A. I., Berger, S., Oorschot, V., Sonntag, C., Rogers, K. L., Marcelle, C., *et al.* (2021) Macrophages provide a transient muscle stem cell niche via NAMPT secretion. *Nature* **591**, 281–287

46. Fu, X., Xiao, J., Wei, Y., Li, S., Liu, Y., Yin, J., Sun, K., Sun, H., Wang, H., Zhang, Z., Zhang, B. T., Sheng, C., Wang, H., and Hu, P. (2015) Combination of inflammation-related cytokines promotes long-term muscle stem cell expansion. *Cell Res.* **25**, 655–673

47. Sacco, A., and Puri, P. L. (2015) Regulation of muscle satellite cell function in tissue homeostasis and aging. *Cell Stem Cell* **16**, 585–587

48. Montarras, D., Morgan, J., Collins, C., Relaix, F., Zaffran, S., Cumano, A., Partridge, T., and Buckingham, M. (2005) Direct isolation of satellite cells for skeletal muscle regeneration. *Science* **309**, 2064–2067

49. Garcia, S. M., Tamaki, S., Lee, S., Wong, A., Jose, A., Dreux, J., Kouklis, G., Sbitany, H., Seth, R., Knott, P. D., Heaton, C., Ryan, W. R., Kim, E. A., Hansen, S. L., Hoffman, W. Y., *et al.* (2018) High-yield purification, preservation, and serial transplantation of human satellite cells. *Stem Cell Rep.* **10**, 1160–1174

50. Lin, C., Han, G., Ning, H., Song, J., Ran, N., Yi, X., Seow, Y., and Yin, H. (2020) Glycine enhances satellite cell proliferation, cell transplantation, and oligonucleotide efficacy in dystrophic muscle. *Mol. Ther.* **28**, 1339–1358

51. Price, F. D., Kuroda, K., and Rudnicki, M. A. (2007) Stem cell based therapies to treat muscular dystrophy. *Biochim. Biophys. Acta* **1772**, 272–283

52. Feige, P., Brun, C. E., Ritso, M., and Rudnicki, M. A. (2018) Orienting muscle stem cells for regeneration in homeostasis, aging, and disease. *Cell Stem Cell* **23**, 653–664

53. Yada, A., Iimuro, Y., Uyama, N., Uda, Y., Okada, T., and Fujimoto, J. (2015) Splenectomy attenuates murine liver fibrosis with hypersplenism stimulating hepatic accumulation of Ly-6C(lo) macrophages. *J. Hepatol.* **63**, 905–916

54. Chen, X., Fang, L., Song, S., Guo, T. B., Liu, A., and Zhang, J. Z. (2009) Thymic regulation of autoimmune disease by accelerated differentiation of Foxp3+ regulatory T cells through IL-7 signaling pathway. *J. Immunol.* **183**, 6135–6144

55. Yamazaki, S., Nishioka, A., Kasuya, S., Ohkura, N., Hemmi, H., Kaisho, T., Taguchi, O., Sakaguchi, S., and Morita, A. (2014) Homeostasis of thymus-derived Foxp3+ regulatory T cells is controlled by ultraviolet B exposure in the skin. *J. Immunol.* **193**, 5488–5497

56. Wei, L., Zheng, Y. Y., Sun, J., Wang, P., Tao, T., Li, Y., Chen, X., Sang, Y., Chong, D., Zhao, W., Zhou, Y., Wang, Y., Jiang, Z., Qiu, T., Li, C. J., *et al.* (2020) GGPP depletion initiates metaflammation through disequilibrating CYB5R3-dependent eicosanoid metabolism. *J. Biol. Chem.* **295**, 15988–16001

57. Qiao, Y. N., He, W. Q., Chen, C. P., Zhang, C. H., Zhao, W., Wang, P., Zhang, L., Wu, Y. Z., Yang, X., Peng, Y. J., Gao, J. M., Kamm, K. E., Stull, J. T., and Zhu, M. S. (2014) Myosin phosphatase target subunit 1 (MYPT1) regulates the contraction and relaxation of vascular smooth muscle and maintains blood pressure. *J. Biol. Chem.* **289**, 22512–22523

58. Gao, Y. Q., Chen, X., Wang, P., Lu, L., Zhao, W., Chen, C., Chen, C. P., Tao, T., Sun, J., Zheng, Y. Y., Du, J., Li, C. J., Gan, Z. J., Gao, X., Chen, H. Q., *et al.* (2015) Regulation of DLK1 by the maternally expressed miR-379/miR-544 cluster may underlie callipyge polar overdominance inheritance. *Proc. Natl. Acad. Sci. U. S. A.* **112**, 13627–13632

59. Chen, X., Gao, Y. Q., Zheng, Y. Y., Wang, W., Wang, P., Liang, J., Zhao, W., Tao, T., Sun, J., Wei, L., Li, Y., Zhou, Y., Gan, Z., Zhang, X., Chen, H. Q., *et al.* (2020) The intragenic microRNA miR199A1 in the dynamin 2 gene contributes to the pathology of X-linked centronuclear myopathy. *J. Biol. Chem.* **295**, 8656–8667

60. Ge, Y., Sun, Y., and Chen, J. (2011) IGF-II is regulated by microRNA-125b in skeletal myogenesis. *J. Cell Biol.* **192**, 69–81

61. Ogura, Y., Hindi, S. M., Sato, S., Xiong, G., Akira, S., and Kumar, A. (2015) TAK1 modulates satellite stem cell homeostasis and skeletal muscle repair. *Nat. Commun.* **6**, 10123

62. Zhang, M., Han, Y., Liu, J., Liu, L., Zheng, L., Chen, Y., Xia, R., Yao, D., Cai, X., and Xu, X. (2020) Rbm24 modulates adult skeletal muscle regeneration via regulation of alternative splicing. *Theranostics* **10**, 11159–11177

63. Liu, J., Huang, Z. P., Nie, M., Wang, G., Silva, W. J., Yang, Q., Freire, P. P., Hu, X., Chen, H., Deng, Z., Pu, W. T., and Wang, D. Z. (2020) Regulation of myonuclear positioning and muscle function by the skeletal muscle-specific CIP protein. *Proc. Natl. Acad. Sci. U. S. A.* **117**, 19254–19265

64. Ding, H., Chen, S., Pan, X., Dai, X., Pan, G., Li, Z., Mai, X., Tian, Y., Zhang, S., Liu, B., Cao, G., Yao, Z., Yao, X., Gao, L., Yang, L., *et al.* (2021) Transferrin receptor 1 ablation in satellite cells impedes skeletal muscle regeneration through activation of ferroptosis. *J. Cachexia Sarcopenia Muscle* **12**, 746–768

65. Gromova, A., Tierney, M. T., and Sacco, A. (2015) FACS-based satellite cell isolation from mouse hind limb muscles. *Bio Protoc.* **5**, e1558

66. Chen, F., Zhou, J., Li, Y., Zhao, Y., Yuan, J., Cao, Y., Wang, L., Zhang, Z., Zhang, B., Wang, C. C., Cheung, T. H., Wu, Z., Wong, C. C., Sun, H., and Wang, H. (2019) YY1 regulates skeletal muscle regeneration through controlling metabolic reprogramming of satellite cells. *EMBO J.* **38**, e99727

67. Wang, L., Chen, X., Zheng, Y., Li, F., Lu, Z., Chen, C., Liu, J., Wang, Y., Peng, Y., Shen, Z., Gao, J., Zhu, M., and Chen, H. (2012) MiR-23a inhibits myogenic differentiation through down regulation of fast myosin heavy chain isoforms. *Exp. Cell Res.* **318**, 2324–2334

68. Ishii, K., Sakurai, H., Suzuki, N., Mabuchi, Y., Sekiya, I., Sekiguchi, K., and Akazawa, C. (2018) Recapitulation of extracellular LAMININ environment maintains stemness of satellite cells in vitro. *Stem Cell Rep.* **10**, 568–582

69. Purushothaman, A. (2019) Exosomes from cell culture-conditioned medium: Isolation by ultracentrifugation and characterization. *Methods Mol. Biol.* **1952**, 233–244

70. Luo, Z., Thorvaldson, L., Blixt, M., and Singh, K. (2019) Determination of regulatory T cell subsets in murine thymus, pancreatic draining lymph node and spleen using flow cytometry. *J. Vis. Exp.* https://doi.org/10.3791/58848